Crack initiation in filled natural rubber: experimental database and macroscopic observations

Elisabeth Ostoja-Kuczynski, Pierre Charrier, Erwan Verron, Gilles Marckmann, Laurent Gornet, Grégory Chagnon

Crack initiation in filled natural rubber: experimental database and macroscopic observations

E. Ostoja Kuczynski & P. Charrier
Modyn Trelleborg, Zone ind. de Carquefou, BP 419, 44474 Carquefou Cedex - France

E. Verron, G. Marckmann, L. Gornet & Chagnon
Ecole Centrale de Nantes, Institut de Recherche en Génie Civil et Mécanique, BP 92101, 44321 Nantes cedex 3, France

ABSTRACT: Nowadays, static and dynamic numerical simulations are widely used during the design loop of new Automotive Anti-Vibration System (AVS) components and the prediction of their fatigue life is a major objective for rubber manufacturers. The definition of an initiation criterion for rubber parts durability must be based on a wide experimental database that should include a large number of different loading conditions. In the present work, two classical test samples are used to develop such an experimental database. In this context, influences of both pre-loading conditions and the non-linear time dependent behaviour of rubber on the fatigue life are highlighted. Then, in regards with these results, an experimental "end-of-life" criterion is established. It is based on AVS component specifications, on macroscopic observations during experiments, and on the evolution of samples global stiffness. In regards with this criterion, Wöhler curves for rubber are proposed and the approach is validated by examining cracks evolution during experiments conducted under different loading conditions.

1 INTRODUCTION

1.1 *Industrial motivation*

Pressure imposed by carmakers on their suppliers is growing: the delivery time for a new car project was previously five years and is now two years. In this context, the numerical simulation should replace experiments in order to sufficiently reduce the design time of new components. Indeed, the development of new products based on a classical iterative design loop is not adapted to the new delivery times.
On one hand, numerical predictions of both static and dynamic responses of new Automotive Anti-Vibration System (AVS) are reliable. On the other hand, the computation of their fatigue life remains a difficult problem. In this context, a fatigue life criterion is a necessary pre-requisite to numerically establish the relevance of technical solutions before their experimental validation.

1.2 *Previous works*

Two major approaches were used to determine the fatigue life of elastomeric parts.

The first approach was introduced by tire manufacturers, and focus on the propagation of an existing defect in the structure. The aim of this type of studies is the determination of the number of cycles that is necessary to propagate the crack until the failure of the part. This approach is based on the tearing energy theory of Rivlin & Thomas (1953). Most of the published papers interested in the fatigue life of rubber parts are using this approach, and some commercial softwares exist. Nevertheless, the propagation study is highly time consuming due to the complexity of finite element simulations; moreover it is not well-adapted to AVS components problems for which structural integrity has to be ensured.

The second approach is better adapted to automotive design offices. It is based on the determination of a Wölher curve that links a fatigue life criterion for the part to a parameter that represents the loading conditions. First published works adopted the maximal principal stretch or the strain energy density as fatigue life criterion. However, these criteria cannot distinguish the fatigue life difference that takes place under uniaxial and biaxial loading conditions (Robert & Benzies 1977). Two recent studies focus on criteria adapted to multiaxial loading conditions. Saintier et al. (2000) proposes to determine the material surface submitted to the maximum tensile loading and to define hardening stresses that characterise the stress state of this surface during unloading. In the same time, Mars (2001) develops another criterion, called the Crack Energy Density (CED), that represents the available tearing energy (to propagate a crack) in a given material plane. This theory leads to different fatigue life val-

ues under uniaxial and multiaxial loading conditions.

Finally, it is to note that the relevance of a crack initiation parameter can be established only with a sufficiently wide experimental database. The aim of the present paper is the development of such a multiaxial database, in order to validate the use of a crack initiation criterion during design studies.

2 EXPERIMENTAL CONTEXT

2.1 *Apparatus*

Two linear and one rotating actuators are used for experiments. They are presented in Figures 1 and 2. Linear actuators are servo-jacks which maximum loading displacements are 50 and 100 mm, and maximum loading speeds are 0.6 $m.s^{-1}$ and 0.3 $m.s^{-1}$, respectively. They can bear a loading of 3 kN. The rotating actuator is an electrical engine having maximum torque and angle of respectively 3 Nm and ± 180°. It is linked with a dynamic torque measurement system (range 2 Nm under 3000 laps per min). Fatigue tests are performed in a climatic chamber, and the temperature is set to 23°C. So, with this equipment, it is possible to realize uniaxial tensile-compressive, torsionnal, and mixed uniaxial tensile / torsion experiments.

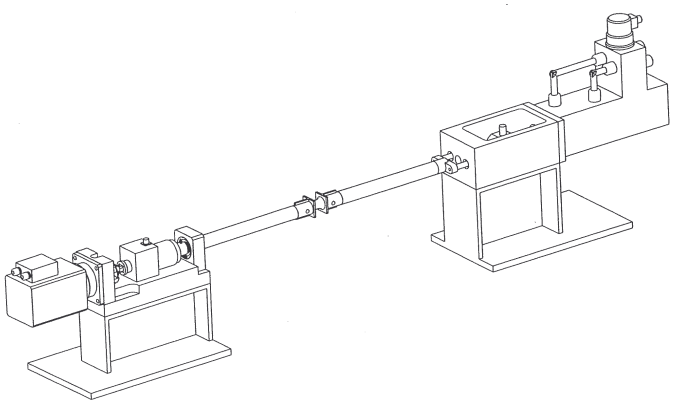

Figure 1. Uniaxial tensile / torsion fatigue experiments. The climatic chamber is not shown.

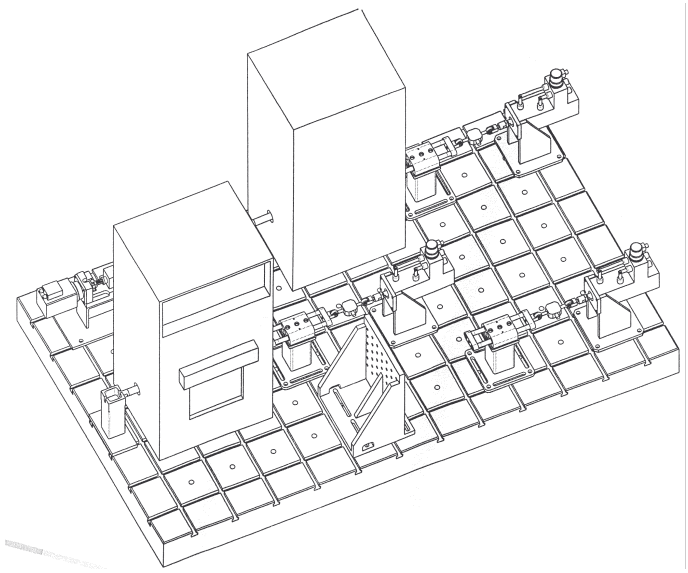

Figure 2. Fatigue experiments room: three linear and one rotating actuators are working together.

2.2 *Samples*

Two classical test samples were used for this experimental campaign. The are presented in Figure 3. The first sample is called a Diabolo sample and is well adapted to uniaxial (tensile and compressive) loading conditions, because the crack initiation zone is localized in the middle of the sample near the surface, and because the local stress state remains approximately uniaxial due to the sample geometry. The second sample is called AE2 sample; it is an axisymmetric notched sample, the radius of the notch being equal to 2 mm. It is used in the case of multiaxial loading conditions, because its geometry induces a very multiaxial stress state in the notch, even under uniaxial loading conditions.

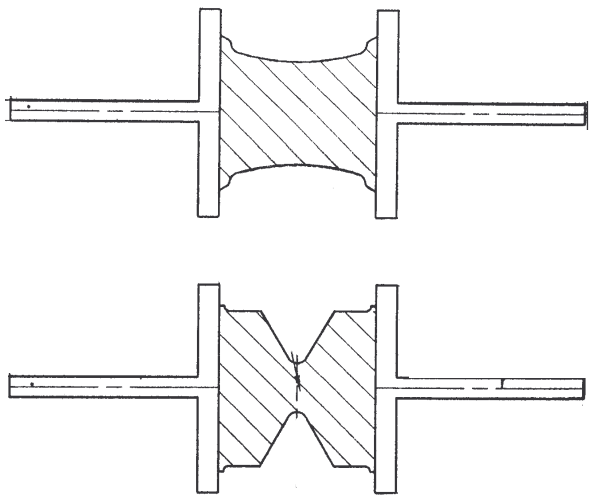

Figure 3. Diabolo sample (upper picture) and AE2 sample (lower picture).

2.3 *Material*

The material studied here is a carbon black-filled natural rubber. Its recipe and mechanical characteristics are given in Table 1.

Table 1: Recipe and mechanical characteristics of the material

Formulation	
NR	100.00
Zinc Oxide	9.85
Plastificant	3.00
Carbon black	34.0
Stearic acid	3.00
Antioxidant	2.00
Accelerators	4.00
Mechanical characteristics	
Density	1.13
Shore hardness A	58
Failure stress (Mpa)	22.9
Failure stretch (%)	635

Samples are obtained by injection moulding in order to reproduce industrial conditions of serial parts. The compound has been cured for 7 min, with a mold temperature set to 160°C. All samples were made using the same material batch to limit properties scattering due for example to mixing. Moreover, in order to overcome aging problems, samples were frozen at –18°C 48 h after their moulding. They are thawed out 24 h before testing.

2.4 *Monitoring and data acquisition*

A specific software was developed to monitor the actuators. Both displacement (resp. angle) and force (resp. torque) can be enforced. A test is a series of cycles sequences that can be sinus of ramp functions. In this way, a large variety of tests can be conducted. As examples, the effect of damage accumulation or of Mullins effect softening on the fatigue life can be explored. Moreover, complex road loading data can be enforced.

The software records cycles data, such as the minimum and maximum displacements and forces, and the shape and area of hysteresis response cycles. Figures 4 and 5 present examples of the evolution of the hysteresis loop obtained for non-relaxing uniaxial tensile experiments on the diabolo sample, respectively under enforced displacement and force loading conditions.

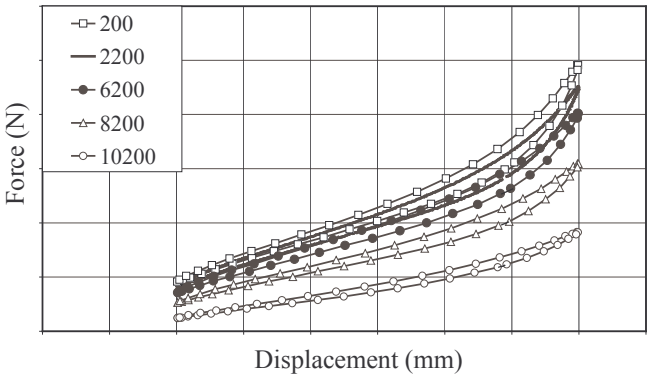

Figure 4. Evolution of the hysteresis loop for an enforced displacement non-relaxing experiment on a diabolo sample. Numbers in the legend stand for the number of cycles.

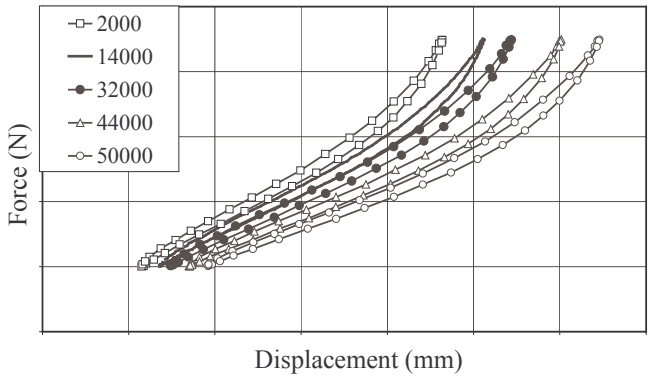

Figure 5. Evolution of the hysteresis loop for an enforced force non-relaxing experiment on a diabolo sample. Numbers in the legend stand for the number of cycles.

3 EXPERIMENTAL RESULTS

3.1 *Temperature near the surface*

A preliminary study was carried out to examine the influence of the experimental frequency on failure mechanisms.

Thus, diabolo samples were subjected to two sinusoidal enforced displacement tests. In both cases, the maximum strain was set to 100% and experiments were conducted in relaxing conditions, i.e. the minimum strain was set to 0. The only difference between the two tests is the frequency. The surface temperature is measured during the experiment using an infrared sensor. First, experiments are carried out at 2 Hz. The surface temperature increases of about 20°C during the test. The cycles number that separates the occurrence of the first macroscopic crack and the sample failure is approximately equal to 25% of the duration of the experiment. After failure, the specimen surface is revealed rough as previously observed by Wang (2002). The failure is due to mechanical fatigue.

Second, similar experiments are conducted with a 10 Hz sinusoidal loading signal. In this case, the increase of surface temperature is approximately equal to 85°C, and the number of cycles between the occurrence of the first defect and the specimen failure is less than 1% of the fatigue life. The broken surface is smooth and brilliant. The failure is due to thermal fatigue.

After this first qualitative result, the measurement of the surface temperature evolution was performed for different loading conditions. An example of such result is presented in Figure 6 as a map of temperature. Then, these results are used to establish an empirical relationship between the displacement amplitude, the loading frequency and the increase of surface temperature, as shown in Figure 7. It has to be noted that the heat build-up does not depend on the mean displacement enforced to the sample.

In the present study, we admit that the increase of surface temperature should not exceed 20°C, and only experimental conditions that satisfy this prerequisite are considered. In that case, the failure is always mechanical, and not thermal. Thus, for a given displacement amplitude Δl, the corresponding loading frequency f is given by:

$$f = \frac{27}{\Delta l} \tag{1}$$

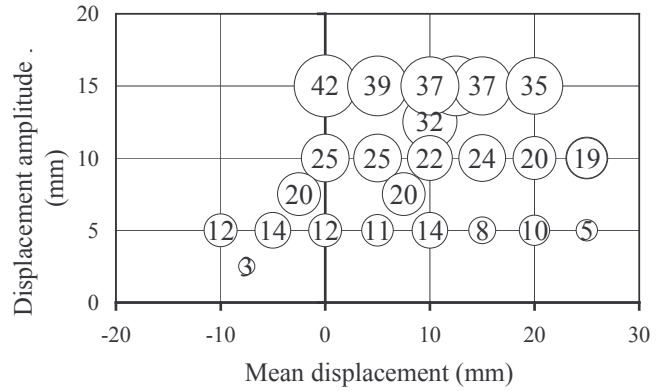

Figure 6. Map of temperature for uniaxial tensile experiments performed at 2 Hz.

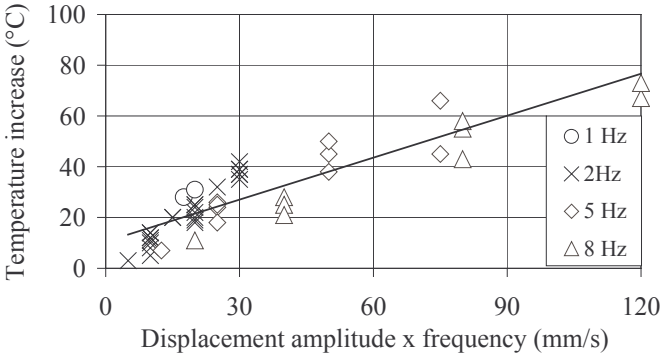

Figure 7. Empirical relationship between the displacement amplitude, the loading frequency and the heat build-up.

3.2 *Experimental determination of the "end of life"*

The experimental determination of a Wöhler curve previously necessitates the definition of a relevant end of life criterion, that does not depend on the deformation state (uniaxial, multiaxial) and on the loading conditions (relaxing, non-relaxing …). In the bibliography, two criteria are proposed. The first one is the number of cycles necessary to break down the sample (see for example Abraham et al. 2001). The second criterion consists in choosing a given decreasing percentage of the maximum force endured by the sample; then, the end of life criterion is the number of cycles corresponding with this force. For example, Mars (2001) consider that the end of life criterion is the number of cycles that corresponds with a loss of 15% of the force measured at the 128th cycle. This criterion was used with our experimental results, as shown in Figure 8. It is demonstrated that this method is not well adapted to elastomers, because of their viscoelastic nature. Indeed, for the samples considered here, the number of cycles obtained by this approach is not significant of a defect size that is independent on the loading level: a 10 mm long crack is observed for small stretch levels, as no crack is detected for medium and high levels. So, a Wöhler curve established by this method lacks of physical meaning in our study.

In the following, a new end of life criterion is used. This criterion does not depend on the deformation state and on the loading level. The effective stiffness of the sample is defined as the ratio between the maximum force and the maximum displacement measured during a cycle:

$$K(N) = \frac{F_{\max}(N)}{L_{\max}(N)} \tag{2}$$

where N is the number of cycle, K is effective stiffness, $F_{\max}$ is the maximum force measured during the cycle N, and $L_{\max}$ is the maximum displacement during this cycle. This criterion has the advantage of being applicable to both enforced displacement and enforced force experiments.

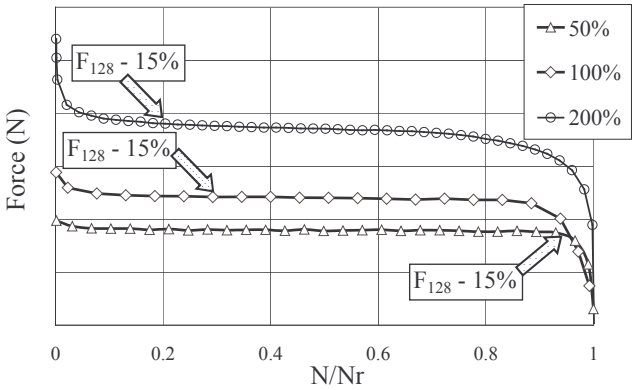

Figure 8. Use of the end of life criterion proposed by Mars (2001) for different loading levels.

This approach exhibits the two physical phenomena that are responsible of the sample loss of stiffness: the viscoelasticity and the growth of a macroscopic defect in the sample. As long as no defect is observed, the stiffness decrease is driven by viscoelasticity and the sample stiffness is simply related to the number of cycles by:

$$K(N) = K_0 \log(N) + B \tag{3}$$

where K_0 and B are material parameters. The differentiation of Equation 3 with respect to N yields:

$$\frac{dK}{dN} = \frac{K_0}{N} \tag{4}$$

Thus, as long as the loss of stiffness is mainly due to viscoelasticity, the simple following equation should be verified:

$$N \cdot \frac{dK}{dN} = \text{cte} \tag{5}$$

Finally, the experimental sample end of life corresponds to the cycle number for which Equation 5 is no more satisfied.

3.3 *Validation of the new end of life criterion*

3.3.1 *Tensile experiments on diabolo samples*

In order to validate the proposed criterion, a uniaxial tensile experiment under relaxing conditions is carried out. Some photographs of the samples are made during the test, in order to detect the occurrence of a defect and its growth until the failure of the sample. The corresponding illustrations are shown in Figure 9. First dots visible with the naked eye take place approximately at the middle of the test (step 1). First, these dots only take place near the surface and are propagating very slowly (steps 2 and 3). Second, the propagation in the sample volume begins when the dots size reaches 2 mm (step 4). Then, propagation accelerates; the crack size represents about one quarter of the sample section (step 5) and finally, the sample breaks down (step 6).

With regards to this analysis, it can be considered that the end of life of a diabolo sample corresponds to the propagation of the defect in the sample volume, i.e. when the crack size is approximately equal to 2 mm. It is very important to note that this critical defect size is not a material intrinsic parameter, because it should be compared with the size of the structure: for example, a 2 mm defect is not relevant for a classical uniaxial dumbbell sample.

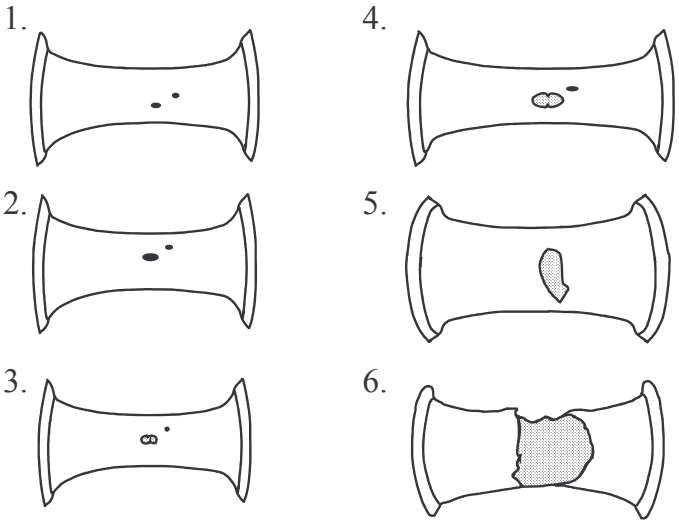

Figure 9. Six steps of the crack growth for a relaxing uniaxial tensile experiment under enforced displacement.

Figure 10 presents both the evolution of the sample stiffness with reference to the problem presented in Figure 9, and the evolution of the developed criterion. The number of cycles reflecting crack initiation (in regards to the present criterion) corresponds to step 4 in Figure 9, i.e. with the real end of life of the structure. Thus, the proposed criterion is validated.

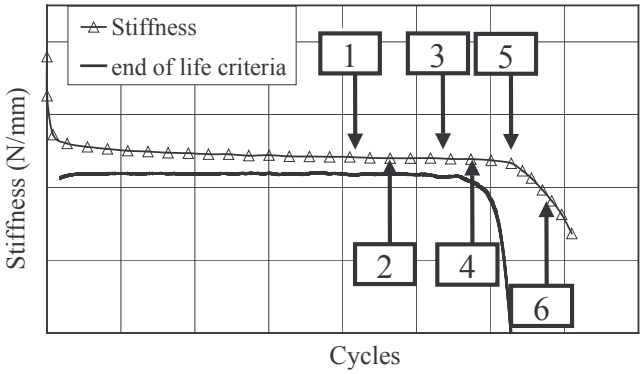

Figure 10. Validation of the experimental end of life criterion using a relaxing uniaxial tensile experiment.

Our criterion does not prejudge the zone of crack initiation, so that it can be used to detect failure both at the surface and in the volume. Figure 11 presents the application of our criterion to a case in which the sample breaks down due to cavitation in the neighbourhood of metallic inserts. It also shows the corresponding failure surface. The crack initiates in the volume and the final failure of the sample is adhesive between the insert and the rubber.

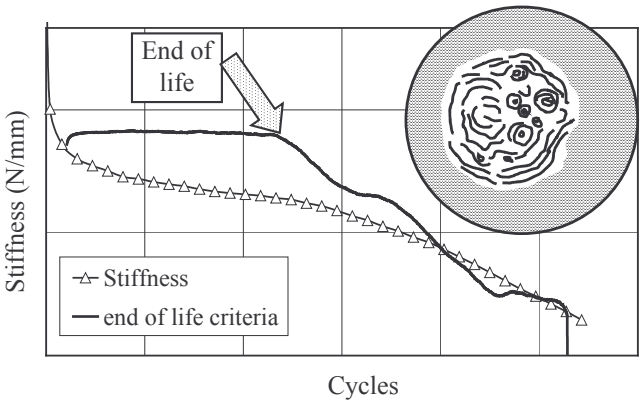

Figure 11. Application of our criterion to a case of cavitation failure. This corresponds to a non-relaxing uniaxial tensile experiment.

Moreover, as our criterion does not involve any decreasing threshold of the sample stiffness, it is also efficient to detect the occurrence of cracks that are propagating parallel to the loading direction, as shown in Figure 12. Indeed, such cracks lead to no decrease of the sample section, contrary to cracks that propagate perpendicular to the loading direction.

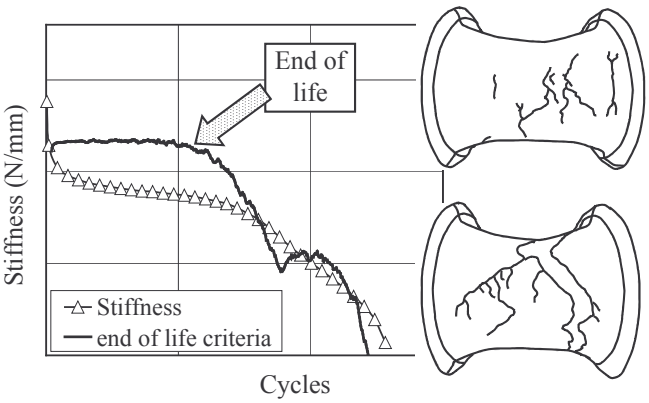

Figure 12. End of life criterion for cracks that propagate parallel to the loading direction. This case corresponds to a non-relaxing uniaxial tensile experiment.

3.3.2 *Torsional experiments on AE2 samples*

In the case of torsional loading conditions, the effective stiffness of the sample is defined as the ratio between the maximum torque and the maximum angle measured during a cycle, similarly to Equation 2.

Some photographs of the sample are made during a relaxing torsional experiment. Figure 13 shows the crack initiation and propagation phenomena, and the evolution of our end of life criterion. As in the previous case, there is a good correlation between the criterion and the crack size: the predicted end of life of the sample corresponds to 1-2 mm cracks.

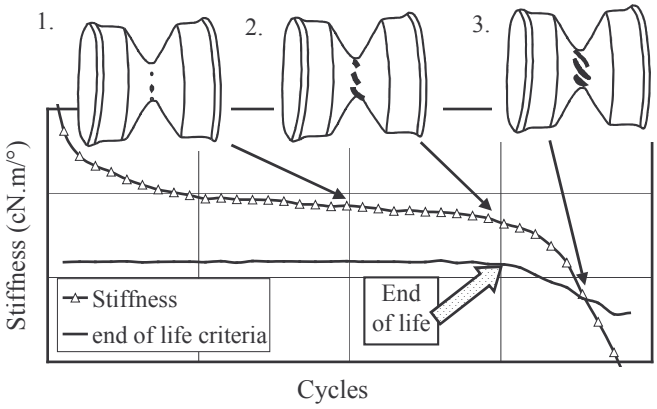

Figure 13. Crack initiation criterion as applied to relaxing torsional loading conditions.

Finally, our approach is validated with an alternated torsional test. As shown in Figure 14, the criterion is revealed to be able to satisfactorily predict the occurrence of 1-2 mm cracks. Note that here, cracks are plane whereas they were inclined for relaxing torsional tests (see above). These observations are not used in the present work, but they will be very useful to validate numerical criteria in which the propagation direction is included.

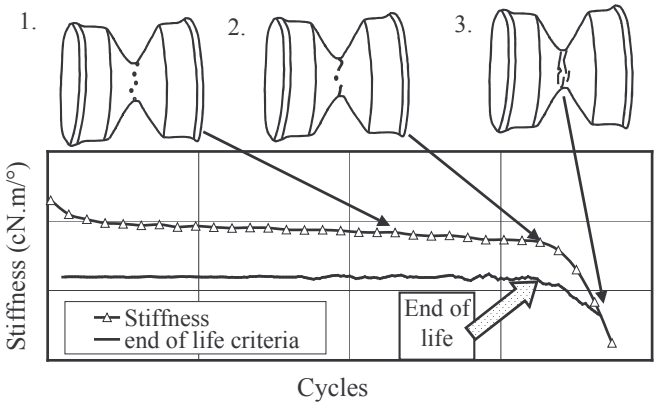

Figure 14. Crack initiation criterion as applied to non-relaxing torsional loading conditions.

3.4 *Determination of a Wölher curve*

The first complete experimental campaign was performed with diabolo samples under relaxing uniaxial tensile tests. The corresponding Wölher curve is presented in Figure 15. The results scattering is low and first applications to industrial parts are satisfactory.

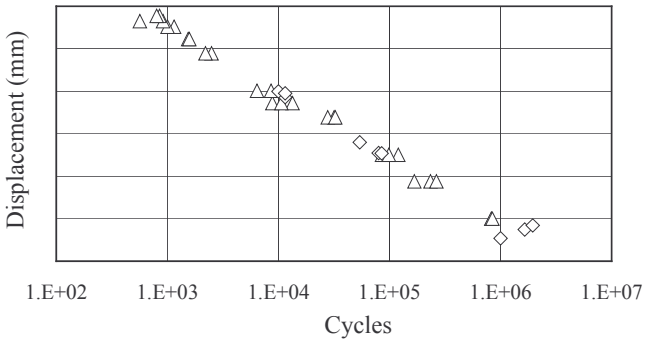

Figure 15. Wölher curve for uniaxial tensile experiments conducted with diabolo samples.

4 CONCLUDING REMARKS

The experimental set-up presented in this paper is sufficiently efficient to validate an end of life criterion for elastomers, including multiaxial effects. In the future, the influence of viscoelasticity and of the mean stress will be examined. The determination of Wölher curves will be highly simplified by taking into account the viscoelastic behaviour of elastomers and more precisely the effect of cyclic relaxation.

REFERENCES

Abraham, F., Alshuth, T. & Jerrams, S. 2001. The dependence of mean stress and stress amplitude of the fatigue life of elastomers. *Proceedings of the International Rubber Conference 2001, 12-14 june 2001, Birmingham, UK.*

Mars, W. V. 2001. *Multiaxial fatigue of rubber*. Ph-D Dissertation, University of Toledo.

Rivlin, R. S. & Thomas, A. G. 1953. Rupture of rubber. I. Characteristic energy for tearing. *J. Polym. Sci. 10 : 291-318.*

Roberts, B. J. & Benzies J. B. The relationship between uniaxial and equibiaxial fatigue in gum and carbon black filled vulcanizates. *Proceedings of the International Rubber Conference 1977, Brighton, UK.*

Saintier, N. , Cailletaud, G. & Piques, R. 2000. Fatigue life prediction of natural rubber component for uniaxial and multiaxial loadings. *In Fracture Mechanics : Applications and Challenges, Proceedings of the 13th European Conference on Fracture, San Sebastian, September 2000.*

Wang, B., Lu, H. & Kim, G. 2002. A damage model for the fatigue life of elastomeric materials, *Mechanics of Materials 34: 475-483.*